Spectroscopic Investigation of the Polymorphism and Side Group Location of Ethylene Copolymers

Zhiqiang Su,[†] Ying Zhao,[†] Yizhuang Xu,[‡] Xiuqin Zhang,[†] Shannong Zhu,[†] Dujin Wang,*[,†] Jinguang Wu,[‡] Charles C. Han,[†] and Duanfu Xu*[,†]

State Key Laboratory of Polymer Physics and Chemistry, Joint Laboratory of Polymer Science and Materials, Institute of Chemistry, The Chinese Academy of Sciences, Beijing 100080, and State Key Laboratory of Rare Earth Materials Chemistry and Applications, College of Chemistry and Molecular Engineering, Peking University, Beijing 100871, China

Received December 7, 2003; Revised Manuscript Received February 8, 2004

ABSTRACT: The polymorphism and side group location of a series of ethylene−vinyl acetate copolymers (EVA) and their hydrolytic products (EVOH) have been investigated by high-resolution cryogenic Fourier transform infrared (FTIR) and nuclear magnetic resonance (NMR) spectroscopy. The experimental results indicated that FTIR spectra can provide direct evidence for side groups entering the crystal lattice of ethylene segments. Through the characterization of the specific IR band variation, it was proved that the hydroxyl group of EVOH enters the crystal lattice, while the side groups of EVA exist predominantly in the amorphous region. The polymorphism and the crystalline phase transformation were investigated for the two series of ethylene copolymers. It was proved that there is only an orthorhombic crystalline phase for all the EVOH copolymers. For EVA copolymers, however, besides the occurrence of a normal orthorhombic crystalline phase, a monoclinic crystalline phase was also detected for the samples with a relatively high content of side groups. The monoclinic crystalline phase is a substable structure and is mainly affected by the content of the side groups and the crystallization conditions. The content of monoclinic crystals does not increase linearly with branching, but to some extent, the increase of the side group content is propitious to the formation of a monoclinic crystalline state. Different heat-treatment methods have great influence on the polymorphism of EVA copolymers. With the increase of the annealing temperature, the monoclinic crystal was gradually transformed to an orthorhombic crystal.

1. Introduction

The crystallization behavior of semicrystalline copolymers is an important and intriguing area of study in the field of polymer research. Many factors, including the composition and sequence distribution of copolymers, the tacticity of the side groups, the hydrogen-bonding interactions between the hydroxyl groups, and the processing conditions, may influence the phase structure of semicrystalline copolymers.[1,2] Without an essentially complete understanding of the crystallization behavior, it is impossible to obtain adequate, predictive structure−property correlations. However, despite extensive investigations, there are still some unsolved problems concerning the crystallization process and the phase structure of the semicrystalline copolymers. Answers for many pendent questions for unorientated ethylene copolymers, such as the location of side groups, the polymorphism, and the phase transformation among different crystalline phases, are needed to understand the crystallization processes, the phase structure, and the resulting material properties.

Two classical models have been established to investigate the location of side groups in semicrystalline polymers, i.e., Flory's exclusion model[3] and Eby's inclusion model.[4] For polyethylene (PE) and ethylene copolymers, the location of side groups in the crystalline phase has been one of the focuses for the investigation of crystalline structures for several decades. Various techniques, including differential scanning calorimetry (DSC), wide-angle X-ray diffraction (WAXD), small-angle X-ray scattering (SAXS), transmission electron microscopy (TEM), nuclear magnetic resonance (NMR) spectroscopy, atomic force microscopy (AFM), etc., have been used for the characterization of the side group location.[5−9] However, none of these methods could provide decisive evidence to demonstrate the incorporation of the side groups into the crystal lattice. Salyer[5] analyzed the melting temperature/composition relationships of ethylene−vinyl acetate copolymers (EVA) and their hydrolytic products (EVOH) and took the change of melting temperature as evidence of hydroxyl groups entering the crystal lattice. Laupretre and co-workers[6] studied random ethylene copolymers with ^{13}C NMR, proposing that small quantities of methyl groups incorporate into the crystalline phase, while side groups larger than a methyl group can hardly be detected in the crystalline phase. Vonk,[7,8] Salyer,[5] and Bunn[9] studied ethylene copolymers (EAc, EVA, LDPE) with WAXD and found that the unit cell dimensions expand and distort with the increase of the side group concentrations. In these investigations, the expansion of the unit cell dimensions was considered as evidence of side groups entering the crystalline phase. However, the dimension variations of the unit cell could not directly demonstrate the incorporation of the side groups into the lattice, because the unit cell dimensions may be affected by the crystalline size, the details of the fold, the fold surface, and the interior defect in the crystals.[10] Infrared spectroscopy, as a powerful tool for the characterization of crystal lattice vibration, has hardly been used for the investigation of the above question, because of the signal-to-noise (S/N) ratio and the resolution of room temperature.

* To whom correspondence should be addressed. E-mail: djwang@iccas.ac.cn (D.W.), xudf@iccas.ac.cn (D.X.).
[†] The Chinese Academy of Sciences.
[‡] Peking University.

10.1021/ma0358576 CCC: $27.50
Published on Web 03/30/2004

Table 1. Basic Parameters of EVA and EVOH Copolymers

sample	comonomer concn wt %	comonomer concn mol %	d/(g/cm^3)	T_m/°C	T_c/°C	MI/(g/10 min)
EVA(9)	9	3.3	0.932	98	88	2
EVA(14)	14	5.0	0.935	88	72	2
EVA(18)	18	6.7	0.940	84	69	3
EVA(28)	28	11.2	0.955	65	52	150
EVA(40)	40	17.8	0.980	49	30	50

It is known that polymorphism is a common phenomenon for orientated ethylene copolymers, but seldom occurs in unorientated ethylene copolymers.[11−13] By using high-resolution FTIR spectroscopy, however, we have previously proven that polymorphism can and does exist in unorientated ethylene copolymers with a long side group and a high side group content, such as poly(ethylene-*co*-dimethylaminoethyl methacrylate) (EDAM) and EVA.[14] However, the mechanism of the polymorphism formation and the transformation among different crystalline phases in the above systems are still not well understood. Recently, we developed a new cryogenic FTIR setup,[15] which can provide a stable low-temperature condition (close to liquid nitrogen temperature), allowing sensitive detection of the variation of crystalline ethylene segments.

As representative ethylene copolymers, EVA and EVOH show various crystallization behaviors under different crystallization conditions or with the variation of compositions, and are frequently used as ideal systems for the investigation of crystallization behavior of semicrystalline polymers. The purpose of this study is to understand the crystallization behavior of EVA and EVOH copolymers, including the location of comonomer units in the crystal lattice, the polymorphism, and the phase transformation among different crystalline phases.

2. Experimental Section

2.1. Materials and Sample Preparation. EVA samples were obtained from the Beijing Organic Chemical Factory, and their physical parameters are listed in Table 1. Melting temperature of each sample was measured using a Mettler DSC 822e differential scanning calorimeter at a heating rate of 10 K/min.

EVOH samples were prepared by homogeneously hydrolyzing EVA in our laboratory. The preparation procedure is described as follows: EVA pellets (5 g) were dissolved completely in toluene at 93 °C. Excessive KOH was dissolved by 2-propanol and was dropped into the EVA−toluene solution slowly. The mixed solution was refluxed for about 10 h. Diluted sulfuric acid solution was used to neutralize residual KOH in the solution. The coarse product was precipitated by a large amount of water. The precipitate was then immersed in water for 24 h, followed by washing with water and drying in the air. To ensure the VA group was converted into a hydroxyl group completely, the hydrolyzing reaction was repeated three times in this work. The hydrolysis degree of the sample was determined by ^{1}H NMR spectroscopy. The results show that the hydrolysis degree of all samples is higher than 98%.

The crystallization procedure and associated thermal history are prime factors in determining the morphological features and physical−mechanical properties of a given polymer. It is not sufficient in terms of sample preparation to consider only the crystallization condition without considering sample size and shape.[16] For example, the actual thermal history of samples with different thicknesses varied greatly. In this work, to ensure the consistency of data measured by FTIR and NMR, the sample films were obtained by a method of two-step melt-pressing; i.e., the samples were first melt-pressed to form a film with a thickness of ca. 100 μm and then submitted for the secondary film-pressing to form the final film with a thickness of ca. 40 μm. The sample was sandwiched between two aluminum flakes. To prevent the sample felt, silicon resin releasing agent was coated on aluminum flakes and was cured at 200 °C. The film-pressing temperature of the samples was 40 °C higher than the melting point of the samples. To investigate the influence of thermal history on the samples, three methods were used to prepare the samples: (1) In the air-cooling method, the samples were obtained by stopping heating to let the molten films cool slowly. (2) In the quenching method, the samples were obtained by immersing the molten films in liquid nitrogen so that the temperature of the samples decreased rapidly. (3) In the annealing method, the samples were obtained by keeping quenched samples for 3 h in a constant-temperature oven at 30, 35, 40, 45, 50, 55, and 60 °C, respectively.

2.2. Measurements. IR spectra of all samples were recorded on a Nicolet Magna 750 FTIR spectrometer with an MCT detector, a 1 cm^{-1} resolution, and 64 scans. To improve the spectral resolution, a cryogenic technique was applied[14,15,17] and the temperature of the samples was controlled at ca. −194 °C during the spectra collection. To prevent the condensation of moisture on the surface of the samples at low temperature, the experiments were carried out in a vacuum.

In the cryogenic IR spectra of EVA and EVOH copolymers, the absorption band of the amorphous fraction is very broad and lies hidden under the two narrow bands. The monoclinic phase also appears as a shoulder overlapped with the other bands. The necessity of using curve-fitting procedures to separate bands and measure their integrated intensities is now apparent. In this work, the curve-fitting program used was reported in our previous work.[18] The deconvoluted peaks can be obtained by using the mixed function of Gauss and Lorentz. The peak numbers and positions are determined by the second-derivative spectra and the deconvolution procedure. Baseline correction is a necessary process before the curve-fitting procedure. The parameter optimization is performed through a least-squares method.

Solid-state NMR experiments were performed on a Bruker AM-300 spectrometer operated at 75.47 MHz at room temperature. The ^{13}C CP/MAS (cross-polarization and magic-angle spinning) technology was adopted to study the phase structure of the ethylene copolymers. The CP parameters were as follows: 90° pulse with a 2 μs width, 1 ms contact time, and 3 s recycle time, 4 mm rotors rotating at 4 kHz, and scan number 2400.

3. Results and Discussion

3.1. Phase Structure of EVA and EVOH. For the investigation of EVA and EVOH copolymers with high-resolution cryogenic FTIR spectroscopy, four absorption bands between 750 and 700 cm^{-1} are commonly used to describe the rocking bands of methylene, among which 733 and 721 cm^{-1} are assigned to the orthorhombic crystalline structure, 724 cm^{-1} is assigned to the amorphous state, and 718 cm^{-1} is assigned to the monoclinic crystalline structure.[19−23]

Figures 1 and 2 show the high-resolution cryogenic FTIR spectra of EVA films prepared with the methods of melt-pressing/quenching and melt-pressing/air-cooling, respectively. It was observed that, at low temperature, the S/N ratios of the IR spectra of EVA were improved significantly and the bandwidths decreased considerably. As a result, the monoclinic band of EVA around 718 cm^{-1}, which can hardly be seen at room temperature, appeared as a shoulder on the right side of the 721 cm^{-1} peak in the cryogenic FTIR spectra with a higher content of side groups. However, no absorbance of a monoclinic crystal was detected for EVA samples with a lower content of side groups. The crystallinity and relative content of the monoclinic crystal for EVA copolymers can be calculated from the following equations:[20,24]

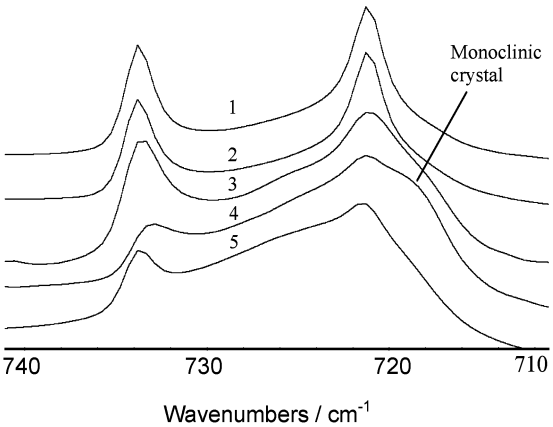

Figure 1. High-resolution cryogenic FTIR spectra of EVA ($\gamma(CH_2)$) with quenching treatment: (1) EVA(9), (2) EVA(14), (3) EVA(18), (4) EVA(28), (5) EVA(40).

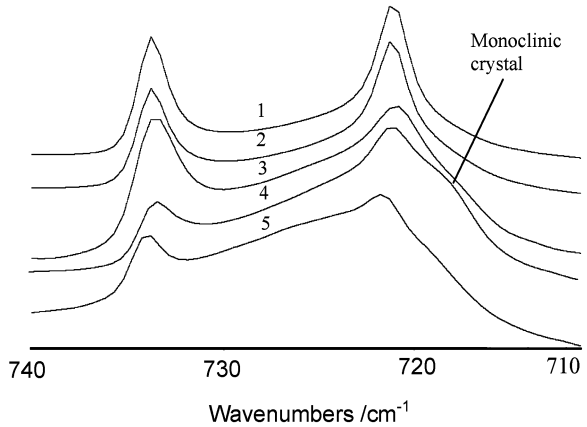

Figure 2. High-resolution cryogenic FTIR spectra of EVA ($\gamma(CH_2)$) with air-cooling treatment: (1) EVA(9), (2) EVA(14), (3) EVA(18), (4) EVA(28), (5) EVA(40).

$$X_c = \frac{I^{obsd}(733 + 721\ cm^{-1})}{I^{obsd}(733 + 721\ cm^{-1}) + \alpha I^{obsd}(724\ cm^{-1})} \quad (1)$$

$$X_c = [I^{obsd}(733 + 721\ cm^{-1}) + \beta I^{obsd}(718\ cm^{-1})](1 - X_{VA})/[I^{obsd}(733 + 721\ cm^{-1}) + \alpha I^{obsd}(724\ cm^{-1}) + \beta I^{obsd}(718\ cm^{-1})] \quad (2)$$

where X_c expresses crystallinity and I^{obsd} represents the observed infrared intensities obtained by curve-fitting techniques. Equation 1 expresses the crystallinity of EVA without a monoclinic crystal. Equation 2 is the crystallinity formula of EVA containing a monoclinic crystal. X_{VA} is the weight percent of the VA unit in EVA copolymers. The coefficient α is the ratio of the molar absorptivity of the crystalline fraction to that of the amorphous fraction, and is defined as

$$\alpha = \frac{I_c^{intr}(733 + 721\ cm^{-1})}{I_a^{intr}(724\ cm^{-1})} \quad (3)$$

where I^{intr} represents the intrinsic intensities. Hagemann found that the value of α is 1.2.[20]

In this paper, we reestimate the value of the coefficient α by infrared measurements on HDPE over the temperature range of 20−160 °C. The HDPE sample was prepared by slow cooling of the HDPE film from the melt to ambient temperature. The obtained film was sandwiched between KBr windows to maintain the same thickness during the heating and cooling procedures. All infrared spectra were measured at a resolution of 1 cm^{-1}. The integrated intensities over the region 750−700 cm^{-1} were plotted against the temperatures. The value of the intrinsic intensity of the amorphous band at ambient temperature, I_a^{intr}(20 °C), one parameter in eq 3, can be estimated. There are two methods for this estimation.[24] The first method is to extrapolate the plot from the molten state to ambient temperature. The results are listed in Table 2. The second method uses the value of the temperature coefficient of the amorphous band, $\partial \ln I_a^{intr}/\partial T$. For PE, it is -1.2×10^{-3} K^{-1}. [20] This leads to a value of 2.23 for I_a^{intr}(20 °C) of our sample. The result is in good agreement with that of the first method. Another parameter in eq 3 is I_c^{intr}(20 °C), the intrinsic intensity of orthorhombic crystalline bands. It can be calculated from Beer's law written in the form

Table 2. Experimental Value of Coefficient α

	20 °C	40 °C		20 °C	40 °C
I^{obsd}(750−700 cm^{-1})	4.04	1.94	I_c^{intr}	4.67	−
I_a^{intr}	2.32[a]	1.94	a	2.1	−
	2.23[b]				

[a] Obtained from the extrapolation method. [b] Calculated from $\partial \ln I_a^{intr}/\partial T$.

$$I_c^{intr}(20\ °C) = \frac{I^{obsd}(750-700\ cm^{-1}, 20\ °C) - (1 - \chi_c)I_\alpha^{intr}(20\ °C)}{\chi_c} \quad (4)$$

The crystallinity(χ_c) in this equation was measured by DSC. For our sample, χ_c was estimated to be 0.74. This leads to a value of 4.67 for I_c^{intr}(20 °C).

According to the above results and eq 3, the value of α is found to be 2.1, which is larger than the previous value of 1.2. The reason for the discrepancy between the two values is still under investigation. We suggest that the error may be introduced in the curve-fitting procedure. Our method is not dependent on such a procedure, so the value we obtained seems more reasonable.

The coefficient β is defined as the ratio of the molar absorption between the orthorhombic and monoclinic crystals in PE. We assume the value of β to be 1, due to the unavailability of this number.

C_m is the ratio of the integrated area of the monoclinic band to that of the whole crystalline bands, corresponding to the relative content of the monoclinic crystal:

$$C_m = \frac{A(718\ cm^{-1})}{A(733 + 721 + 718\ cm^{-1})} \quad (5)$$

The above calculated results indicate that the whole crystallinity of EVA copolymers decreases with branching (Figure 3). It was observed that the crystallinity of air-cooled samples is larger than that of quenched ones, implying an enhancing effect of the air-cooling treatment on the crystallinity of EVA copolymers. Another interesting phenomenon is that quenching treatment led to prior formation of a monoclinic crystal, which can also be confirmed by ^{13}C CP/MAS NMR spectra. The NMR results will be discussed in detail later.

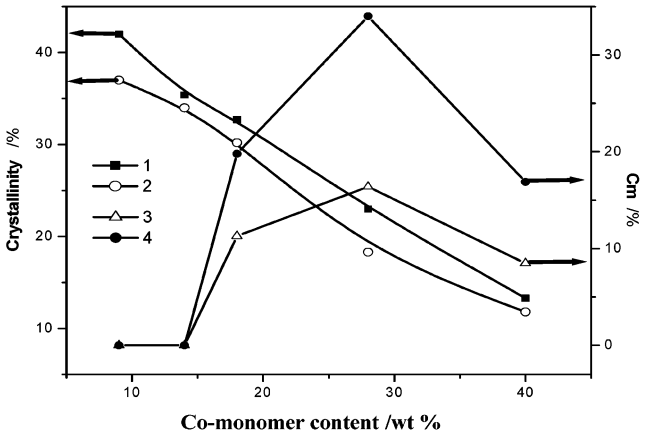

Figure 3. Crystallinity and relative content of a monoclinic crystal of EVA under different crystallization conditions as a function of VA content: (1) crystallinity of air-cooled samples, (2) crystallinity of quenched samples, (3) C_m of air-cooled samples, (4) C_m of quenched samples.

All these results indicate that the content of the comonomer unit influences not only the crystallinity but also the crystalline phase of EVA copolymers, which can be explained by the fact that the long side groups of EVA block the ethylene segments' movement in the crystallization process and affect the ordered packing of the ethylene segments. In such a case, the monoclinic crystalline structure may become thermodynamically stable or dynamically favored. Another possible explanation is that the average sequence length of crystallized ethylene segments is shortened with an increase of the side group content, which, accordingly, induces a decrease of the crystallization ability of ethylene segments. So, the relative content of the stable orthorhombic phase decreases, while that of the substable monoclinic crystal and the amorphous phase increases with branching. Quenching treatment made the ethylene segments freeze in an ultrashort time; therefore, many molecular chains cannot be adjusted to the lowest energy state (orthorhombic crystal) and are confined to be thermodynamically substable (monoclinic crystal). A similar conclusion about the monoclinic crystal formation in ethylene−butene and ethylene−octene copolymers has also been obtained by Hu and Sirota.[25]

It should be pointed out that the content of monoclinic crystals does not increase linearly with branching. The monoclinic crystal percentage of EVA(28) is the largest among all the EVA samples. For ethylene copolymers, the monoclinic crystal is a transitional structure from a spherical crystal to a fibrosis structure. It is a substable crystalline phase and forms under special conditions,[26,27] which can be transformed to an orthorhombic crystal gradually when the environmental temperature is close to the crystallization point. As shown in Table 1, the T_m and T_c of EVA copolymers decrease with increasing VA content. The T_c values of EVA(18) and EVA(28) are 70 and 52 °C, respectively, while that of EVA(40) is near 30 °C, close to room temperature. In this work, the samples were kept in a desiccator at room temperature before testing. At room temperature, monoclinic crystals of EVA (40) will be partly transformed to orthorhombic crystals, leading to a relative decrease of the monoclinic crystal content of EVA(40), compared with that of EVA(28).

Figures 4 and 5 show the cryogenic FTIR spectra of EVOH copolymers quenched and air-cooled, respectively. Whether the samples are quenched or air-cooled, the monoclinic IR band cannot be detected. In the second-derivative spectra of $\gamma(CH_2)$ bands of a series of EVOH, only two bands (733 and 721 cm^{-1}) were observed, confirming the unique existence of an orthorhombic phase. Compared with EVA, the hydroxyl group of EVOH is much smaller than the VA group. Its steric hindrance effect on the ethylene segments' movement is very small. Meanwhile, interchain interactions also have an important effect on the formation of a condensed-state structure. The intermolecular hydrogen bonds among the hydroxyl groups enhance the interaction between chain segments. All these factors make the phase structure of EVOH differ from that of EVA. To further understand the polymorphism and phase structure of ethylene copolymers, solid ^{13}C NMR measurements were carried out for both EVA and EVOH.

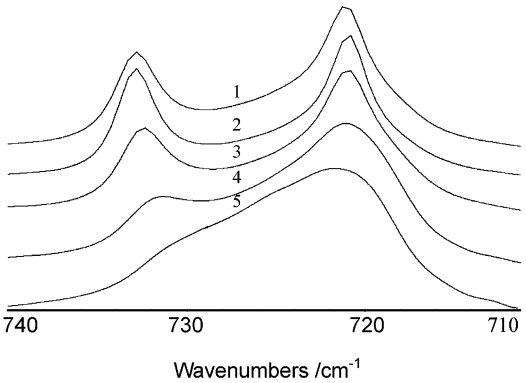

Figure 4. High-resolution cryogenic FTIR spectra of EVOH ($\gamma(CH_2)$) with quenching treatment: (1) EVOH(9), (2) EVOH-(14), (3) EVOH(18), (4) EVOH(28), (5) EVOH(40).

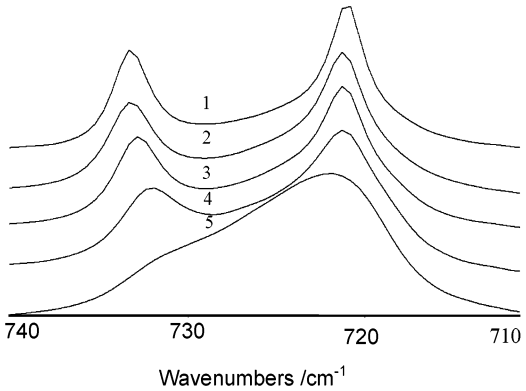

Figure 5. High-resolution cryogenic FTIR spectra of EVOH ($\gamma(CH_2)$) with air-cooling treatment: (1) EVOH(9), (2) EVOH-(14), (3) EVOH(18), (4) EVOH(28), (5) EVOH(40).

Recently, high-resolution solid-state ^{13}C NMR spectroscopy has been used to study the morphology and structure of semicrystalline polymers by combining techniques of MAS, high-power proton decoupling, and CP excitation.[28−34] As reported previously,[35−37] on the basis of ^{13}C spin−spin relaxation time measurements and line shape analysis, the ^{13}C CP/MAS spectrum of PE consists of a crystalline region signal and a noncrystalline region signal. Because the crystalline phase of ethylene copolymers is mainly composed of ethylene segments, the ^{13}C NMR spectra of the samples can also be well resolved into the crystalline and amorphous contributions. The total spectrum has been analyzed in terms of Lorentzian functions centered at 33.4 ppm (monoclinic crystal), 33.0 ppm (orthorhombic crystal),

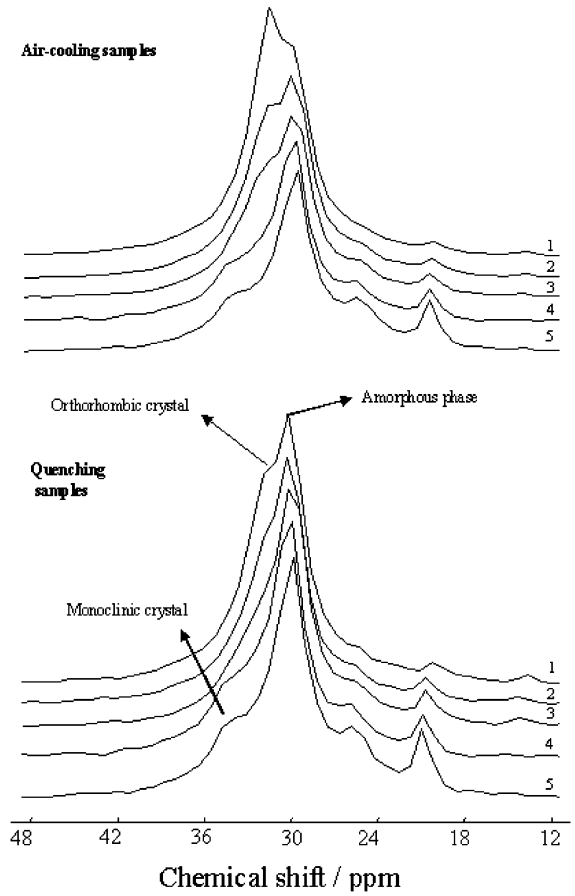

Figure 6. ^{13}C CP/MAS NMR spectra of EVA copolymers under different crystallization conditions: (1) EVA(9), (2) EVA-(14), (3) EVA(18), (4) EVA(28), (5) EVA(40).

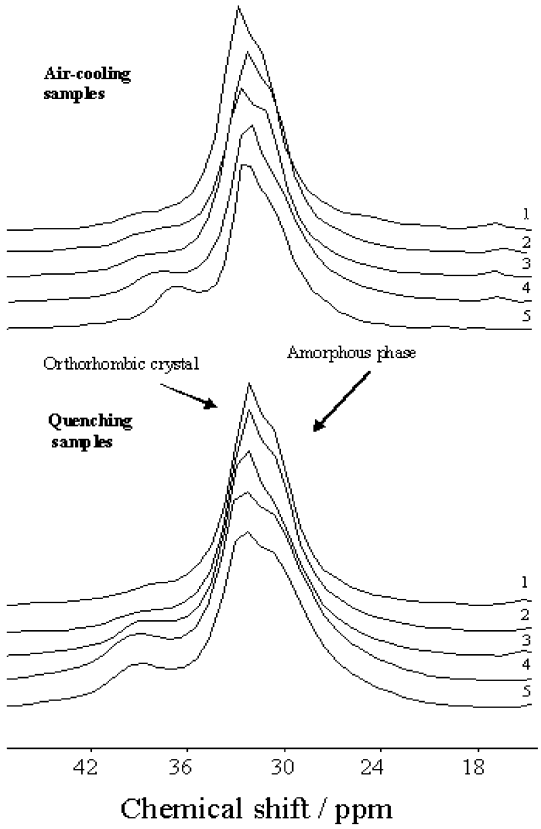

Figure 7. ^{13}C CP/MAS NMR spectra of EVOH copolymers under different crystallization conditions: (1) EVOH(9), (2) EVOH(14), (3) EVOH(18), (4) EVOH(28), (5) EVOH(40).

and 31.0 ppm (amorphous component), on the basis of the results obtained for short T_{1c} components.

Figures 6 and 7 are the ^{13}C CP/MAS NMR spectra of the EVA and EVOH samples under different crystallization conditions, respectively. The signals of the monoclinic phase are quite apparent and can be distinguished easily from the NMR spectra of EVA samples with a higher content of side groups. In the spectra of EVA with a lower side group content and EVOH copolymers, however, the signals of the monoclinic phase cannot be observed, whether they are quenched or air-cooled samples. For the purpose of obtaining more detailed information about the crystalline and amorphous components, the curve-fitting results of EVA(28) and EVOH(28) are given as examples in Figures 8 and 9, respectively. These results are in good agreement with the conclusion obtained from the high-resolution cryogenic FTIR spectra. The difference in phase structure of EVA and EVOH originates from the difference in their side groups. The hydroxyl groups of EVOH have smaller steric hindrance and interaction between chain segments exists, which result in the different crystalline behaviors of the two kinds of samples.

3.2. Transformation between Different Crystalline Phases of EVA. On the basis of the above observations and discussion, a conclusion can be drawn that polymorphism exists in unorientated EVA films with a higher content of side groups. To better understand the polymorphism of ethylene copolymers, the phase transformation from monoclinic to orthorhombic was investigated under different annealing tempera-

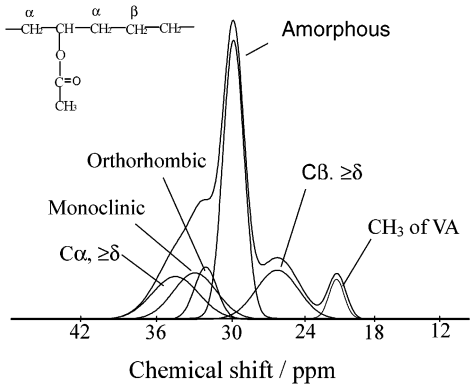

Figure 8. Component analysis of ^{13}C CP/MAS NMR spectra of EVA(28).

tures for EVA(28). A series of EVA(28) samples were annealed for 3 h at 30, 35, 40, 45, 50, 55, and 60 °C. The aim is to transform a monoclinic crystal to an orthorhombic crystal as fully as possible, and to study the influence of thermal history on the crystalline transformation.

Figure 10 shows the second-derivative spectra of the CH_2 rocking vibration of EVA(28) under different annealing temperatures. The variation of different crystalline bands is distinct. With increasing annealing temperature, the 718 cm^{-1} band disappeared at 60 °C, and only the 721 and 733 cm^{-1} bands were left. Curve-fitting results indicated that the relative content of the monoclinic crystal gradually decreases with increasing annealing temperature while the orthorhombic crystal content increases (Figure 11). This result implied that the increased mobility of the polymer chains at high

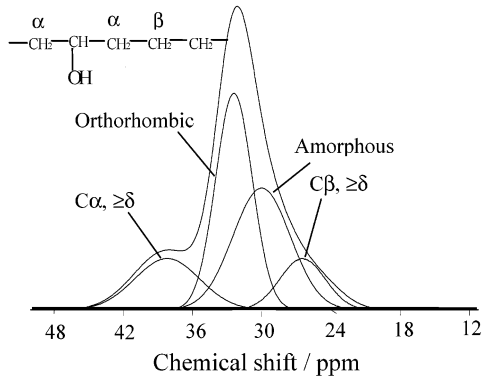

Figure 9. Component analysis of ^{13}C CP/MAS NMR spectra of EVOH(28).

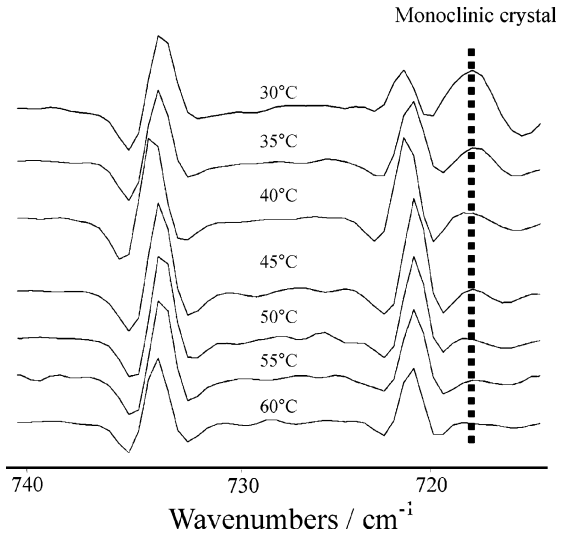

Figure 10. Second-derivative FTIR spectra of EVA(28) ($\gamma(CH_2)$) under different annealing temperatures.

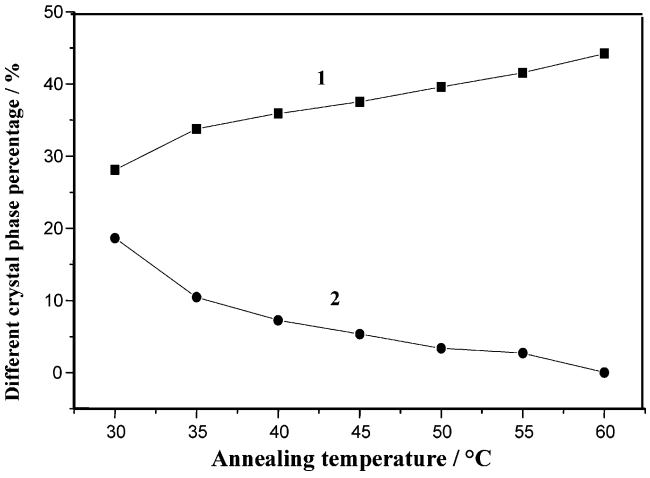

Figure 11. Relative content of the monoclinic and orthohombic phases in EVA copolymers under different annealing temperatures: (1) orthorhombic crystalline phase content, $A(733 + 721\ cm^{-1})/A(733 + 724 + 721 + 717\ cm^{-1})$, (2) monoclinic crystalline phase content, $A(717\ cm^{-1})/A(733 + 724 + 721 + 717\ cm^{-1})$.

temperature induces the rearrangement of the crystalline ethylene segments, and consequently causes the gradual transformation from a monoclinic crystal to an orthorhombic crystal. When the annealing temperature is increased to a certain value (60 °C), the monoclinic crystal disappears completely.

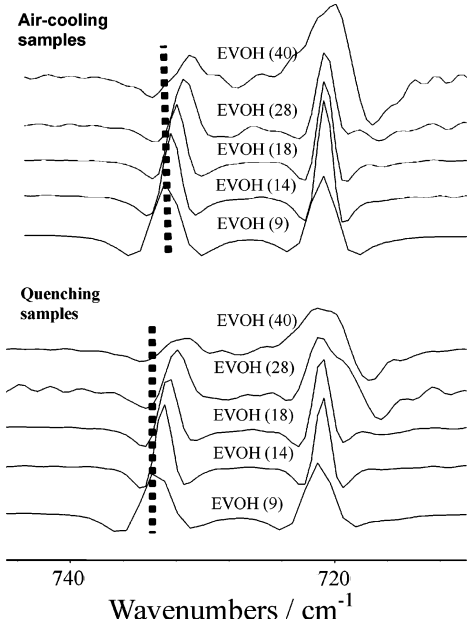

Figure 12. Second-derivative FTIR spectra of EVOH copolymers ($\gamma(CH_2)$) with different comonomer contents under different crystallization conditions.

3.3. Location of the Side Groups of EVOH and EVA. We have just discussed the effect of crystallization conditions and side group content on the IR spectra of EVA and EVOH copolymers from the viewpoint of polymorphism and crystalline phase transformation. The second-derivative spectra may give more detailed information about the crystallization characteristics of ethylene copolymers. It was found from the second-derivative spectra of EVOH copolymers that the peak position of the 733 cm^{-1} band for both air-cooled and quenched samples all gradually shifted to lower frequencies with branching while that of the 721 cm^{-1} band remained almost unchanged (Figure 12). With the increase of the side group content from 9% to 40%, the maximum peak shifts of the 733 cm^{-1} band for both air-cooled and quenched samples are 2.1 and 3.0 cm^{-1}, respectively. As the resolution of the spectra is 1 cm^{-1}, such a band shift from 733 to 730 cm^{-1} here is reliable.

The band shift of the rocking vibration for EVOH copolymers directly reflects the change of crystallinity, which is mainly affected by the location of the side group as the other crystallization conditions were kept unchanged. If the hydroxyl groups enter the crystal lattice, the ordered packing of the ethylene segments will be disrupted, and the crystalline state will be inevitably influenced, which is closely related with the IR band shift. Crystallization perfection will lead to the "blue shift" of the rocking band of the ethylene segments. The higher hydroxyl group content in EVOH copolymers provides higher opportunities for hydroxyl groups to be included in the crystal lattice, which in turn causes the imperfection of crystallinity and the "red shift" of the crystalline bands from 733.8 to 731.7 cm^{-1} for air-cooled samples, and from 733.8 to 730.8 cm^{-1} for quenched samples.

Figure 12 also indicated that the effect of quenching treatment on the band shift is larger than that of air-cooling treatment. Under air-cooling conditions, the crystallization rate of EVOH copolymers is relatively slow and the ethylene segments can pack into a more ordered structure, so fewer hydroxyl groups can enter

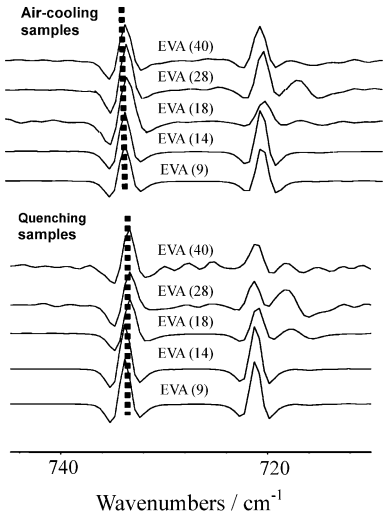

Figure 13. Second-derivative IR spectra of EVA copolymers ($\gamma(CH_2)$) under different crystallization conditions.

the crystalline region. On the contrary, when the samples are quenched, most of the ethylene segments do not have enough time to adjust themselves to a stable state and are fixed without well-regulated packing. As a result, more hydroxyl groups have the opportunity to enter the crystalline region. Therefore, the band shift of the crystalline region of quenched samples is larger than that of the crystalline region of air-cooled samples. All the above analysis and discussion indicated that the IR band shift of the crystalline region provides direct evidence for hydroxyl groups entering the crystal lattice of ethylene segments.

The 733 cm^{-1} band for EVA copolymers, however, was found not to vary with branching, indicating that VA groups do not enter the crystalline region (Figure 13), whether the samples were air-cooled or quenched. This result can be considered as further evidence for the OH group entering the crystal lattice from an opposite point of view.

The peak position difference between the 733 and 721 cm^{-1} bands, as well as the half-width of the 733 cm^{-1} band, is also correlated with the crystallinity perfection for ethylene copolymers. A larger 733 cm^{-1}/721 cm^{-1} band difference and narrower half-width of the 733 cm^{-1} band correspond to a more ordered crystalline structure. Whether the samples are quenched or air-cooled, the 733 cm^{-1}/721 cm^{-1} band differences of the EVA samples remain constant with branching while the 733 cm^{-1}/721 cm^{-1} band differences of the EVOH samples decrease with branching (Figure 14), which also proves the fact that the crystallization of ethylene segments of EVA copolymers was not disturbed by the content of the side groups. On the contrary, the crystallization of EVOH copolymers was influenced by the content of OH groups; i.e., a higher side group content in copolymers resulted in more OH groups being included in the crystal lattice and consequently more lattice deformation. As a result of the OH groups entering the crystal lattice, the 733 cm^{-1}/721 cm^{-1} band difference is decreased. The variation of the half-width of EVA and EVOH copolymers with branching (Figure 15) gives further evidence that the crystallinity perfection of EVOH samples is weaker than that of EVA samples, due to the side group entering the crystalline region.

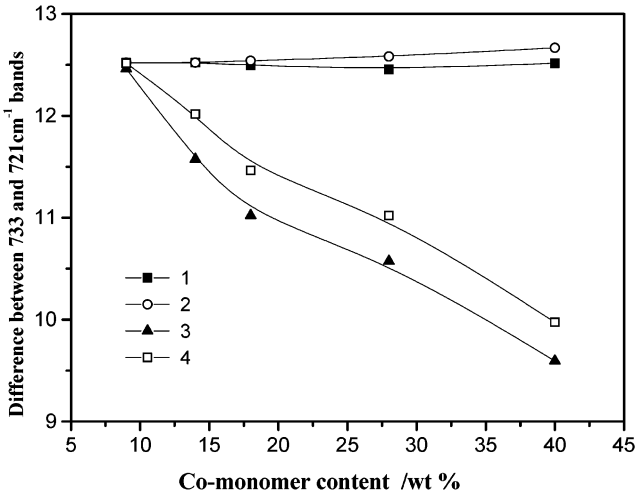

Figure 14. Variation of the difference between the 733 and 721 cm^{-1} bands as a function of the comonomer content: (1) quenched EVA samples, (2) air-cooled EVA samples, (3) quenched EVOH samples, (4) air-cooled EVOH samples.

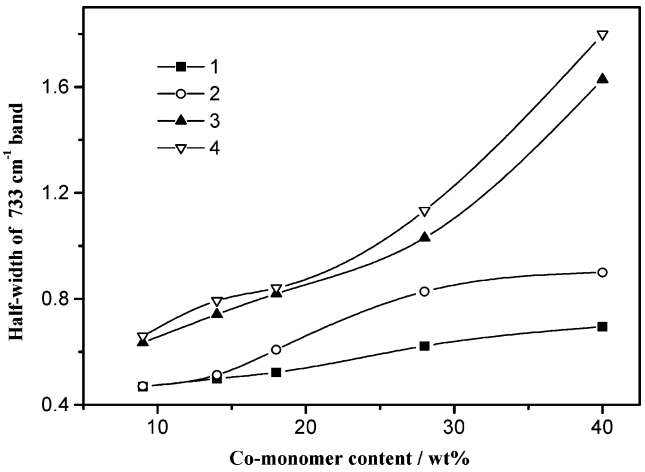

Figure 15. Relationship between the half-width of the 733 cm^{-1} band and the comonomer content: (1) air-cooled EVA samples, (2) quenched EVA samples, (3) air-cooled EVOH samples, (4) quenched EVOH samples.

4. Conclusions

The polymorphism and side group location of a series of EVA and EVOH copolymers have been investigated by high-resolution cryogenic FTIR and solid-state NMR spectroscopy. The FTIR spectra's resolution and sensitivity are greatly enhanced. The polymorphism, crystalline phase transformation, and side group location were characterized by detailed analysis of the IR bands of the rocking vibration of ethylene segments in both EVA and EVOH copolymers, and the following conclusions can be drawn.

(1) Besides the stable orthorhombic crystal, a monoclinic crystal was also formed in the crystalline region of EVA with a higher content of side groups. Increasing the side group content and quenching treatment help the formation of the monoclinic crystal. For EVOH copolymers, however, whether the samples are quenched or air-cooled, the monoclinic band cannot be detected in the crystalline region with high-resolution cryogenic FTIR spectroscopy. The same results were obtained with ^{13}C CP/MAS NMR spectroscopy. Up to now, the relationship between the polymorphism and the chain structure of unorientated ethylene copolymers has not

been systematically established; the findings of our work are beneficial for better understanding of the crystallization behavior of ethylene copolymers.

(2) The transformation from a monoclinic crystal to an orthorhombic crystal was observed for EVA copolymers, which were annealed at different temperatures. The substable monoclinic crystal was gradually transformed to an orthorhombic crystal with increasing annealing temperature.

(3) With direct evidence of the IR band shift of the rocking vibration (733 cm^{-1}) of ethylene segments, it was proved that the hydroxyl groups of EVOH enter the crystalline region while the side groups of EVA copolymers exist predominantly in the amorphous region. So, high-resolution cryogenic FTIR spectroscopy is a powerful technique for characterization whether the side groups of the ethylene copolymers enter the crystal lattice or not.

Acknowledgment. This work was partly supported by the National Natural Science Foundation of China (NSFC; Grant No. 50290090), Polymer Science and Materials Team Building Project, and Directional Project from CAS.

References and Notes

(1) Zhang, Q. J.; Lin, W. X.; Chen, Q.; Yang, G. *Macromolecules* **2000**, *33*, 8904.
(2) Takahashi, M.; Tashiro, K.; Amiya, S. *Macromolecules* **1999**, *32*, 5860.
(3) Flory, P. J. *Trans. Faraday Soc.* **1955**, *51*, 848.
(4) Eby, R. K. *J. Appl. Phys.* **1963**, *34*, 2442.
(5) Salyer, I. O.; Kenyon, A. S. *J. Polym. Sci., Part A-1* **1971**, *9*, 3083.
(6) Laupret, F.; Monnerie, L.; Barthelemy, L.; Vairon, J. P.; Sanzeau, A.; Roussel, D. *Polym. Bull.* **1986**, *15*, 159.
(7) Vonk, C. G.; Pijpers, A. P. *J. Polym. Sci., Polym. Phys. Ed.* **1985**, *23*, 2517.
(8) Vonk, C. G. *J. Polym. Sci., Polym. Phys. Ed.* **1985**, *23*, 2539.
(9) Bunn, C. W. In *Fibers from Synthetic Polymers*; Hill, R., Ed.; Elsevier: New York−Amsterdam, 1953.
(10) Davis, G. T.; Eby, R. K.; Martin, G. M. *J. Appl. Phys.* **1968**, *39*, 4973.
(11) Liu T. M.; Juska, T. D.; Harrisom, I. R. *Polymer* **1986**, *27*, 247.
(12) Saraf, R. F.; Porter, R. S. *J. Polym. Sci., Polym. Phys. Ed.* **1988**, *26*, 1049.
(13) Yan, R. J.; Jiang, B. Z. *J. Polym. Sci., Part B: Polym. Phys.* **1993**, *31*, 1089.
(14) Kang, N.; Xu, Y. Z.; Wu, J. G.; Feng, W.; Weng, S. F.; Xu, D. F. *Phys. Chem. Chem. Phys.* **2000**, *2*, 3627.
(15) Kang, N.; Xu, Y. Z.; Weng, S. F.; Wu, J. G.; Xu, D. F.; Xu, G. X. *The Pittsburgh Conference 51th Anniversary*; p 1768.
(16) Axelson, D. E. In *High-resolution NMR Spectroscopy of Synthetic Polymers in Bulk*; Komoroski, Ed.; 1986; p 157.
(17) Kang, N.; Xu, Y. Z.; Cai, Y. L.; Xu, D. F.; Xu, J. G.; Xu, G. X. *J. Mol. Struct.* **2001**, *562*, 19.
(18) Xu, Y. Z.; Li, W. H.; Peng, Q.; Xu, Z. H.; Weng, S. F.; Song, Z. F.; Wu, J. G.; Xu, G. X. *Spectrosc. Spectral Anal.* **1997**, *17*, 55.
(19) Hagemann, H.; Strauss, H. L.; Snyder, R. G. *Macromolecules* **1987**, *30*, 2810.
(20) Hagemann, H.; Snyder, R. G.; Peacock, A. J.; Mandelkern, L. *Macromolecules* **1989**, *22*, 3600.
(21) Zhang, H. P.; Xu, D. F.; Xu, Y. Z.; Weng, S. F.; Wu, J. G. *Mikrochim. Acta (Suppl.)* **1997**, *14*, 425.
(22) Snyder, R. G. *J. Chem. Phys.* **1979**, *71*, 3229.
(23) Snyder, R. G.; Maroncelli, M.; Strauss, H. L.; Hallmark, V. M. *J. Phys. Chem.* **1986**, *90*, 5623.
(24) Zhang, H. P.; Xu, D. F.; Yang, J. Y. *International Miarosymposium on Polymer Physics*, 1995; Xi'an, p 32.
(25) Hu, W.; Sirota, E. B. *Macromolecules* **2003**, *36*, 5144.
(26) Peterlin, A. *J. Mater. Sci.* **1971**, *6*, 490.
(27) Juska, T.; Harrison, R. *Polym. Eng. Rev.* **1982**, *2*, 14.
(28) Andrew, E. R. *Prog. Nucl. Magn. Reson. Spectrosc.* **1971**, *8*, 1.
(29) Schaefer, J.; Stejskal, E. O.; Buchdahl, R. *Macromolecules* **1975**, *8*, 291.
(30) Schaefer, J.; Stejskal, E. O.; Buchdahl, R. *Macromolecules* **1977**, *10*, 384.
(31) Garroway, A. N.; Moniz, W. B.; Resing, H. A. *ACS Symp. Ser.* **1978**, No. 103.
(32) Vanderhart, D. L.; Perez, E. *Macromolecules* **1986**, *19*, 1902.
(33) Kitamaru, R.; Horii, F.; Murayama, K. *Macromolecules* **1986**, *19*, 636.
(34) Zhang, Q. J.; Lin, W. X.; Yang, G.; Chen, Q. *J. Polym. Sci., Part B: Polym. Phys.* **2002**, *40*, 2199.
(35) Kitamaru, R.; Horii, F.; Zhu, Q.; Bassett, D. C.; Olley, R. H. *Polymer* **1994**, *35*, 1171.
(36) Nakagawa, M.; Horii, F.; Kitamaru, R. *Polymer* **1990**, *31*, 323.
(37) Luo, H. J.; Chen, Q.; Yang, G.; Xu, D. F. *Polymer* **1998**, *39*, 943.

MA0358576